Chapter

CONCLUSION/DISCUSSION

The global scale energy fluxes in the climate system can be understood in terms of the spatio/temporal gradients of the energy entering the system (ASR) and the relative efficiencies of energy export. In Chapter 2, we demonstrated that, in the hemispheric average, ASR is primarily controlled by cloud reflection and only secondarily by surface reflection. In Chapter 3, we demonstrated that the equator-to-pole contrast of ASR (ASR^*) is also primarily controlled by atmospheric reflection (and varies significantly between models). Unsurprisingly, the same processes that control the global average ASR also control the meridional structure of ASR and thus the large scale forcing of the atmospheric and oceanic circulation in the climate system.

The equator-to-pole contrast of energy entering the climate system (ASR^*) must be balanced by the equator-to-pole gradient of energy radiated to space (OLR^*) and the energy transported between the tropics and extratropics (MHT_{MAX}) in an equilibrium system; the surplus of energy entering the tropics (relative to the global average) must be ameliorated by the sum of radiative and dynamic energy exports. As such, the ratio of MHT_{MAX} to OLR^* is equal to the relative efficiency of dynamic and radiative energy export on the equator-to-pole scale (hereafter,δ) and is of order 2 in both the observations and the models (Table **??**). This suggests that dynamic energy export is a more efficient pathway toward achieving equilibrium on the equator-to-pole scale as compared to radiative energy export. It is therefore unsurprising that the large inter-model spread in ASR^* is primarily balanced by model differences in MHT_{MAX} and only secondarily by model differences in OLR^* (Chapter 3). In terms of the inter-model spread, a typical ASR^* anomaly is balanced by $MHT_{MAX}$and OLR^* anomalies in a ratio of approximately 2:1 (as assessed by the regression coefficients between MHT_{MAX}/OLR^* and ASR^* – Table **??**). Thus, given the inter-model spread in ASR^* (from clouds), the inter-model spread in $MHT_{MAX}$and OLR^*

behaves as we would expect based on the relative energy export efficiencies diagnosed from the observed climatology.

More formally, we can understand the conclusions reached in Chapter 3 in terms of the energy export efficiencies introduced in Chapter 4. In the annual average, the MHT_{MAX} into the extratropics in each climate model is equal to

$$MHT_{MAX} = ASR * \frac{MHT_{MAX}}{MHT_{MAX} + OLR*} \approx ASR * \frac{\delta}{\delta + 1}. \tag{1.1}$$

The first equality holds because the denominator of the middle expression is equal to $ASR*$ by Equation **??**. In the second approximate equality, δ is the ratio of the dynamic and radiative energy export efficiencies. In the annual average,

$$\delta = \frac{2B_{MHT}}{B_{OLR}} \approx \frac{MHT_{MAX}}{OLR*}, \tag{1.2}$$

(Chapter 4) and the near equality holds if both the $OLR*$ and MHT_{MAX} are linear functions of the temperature gradient. These equations provide a crucial link between the concepts discussed in Chapter 4 and the results presented in Chapter 3.

Equation 1.1 demonstrates that inter-model differences in $MHT_{MAX}$are a consequence of inter-model differences in $ASR*$ or the relative efficiencies of the dynamic and radiative energy exports. We now explore the expected behavior of the inter-model spread in MHT_{MAX} in the hypothetical limits of model invariant $ASR*$ ("Limiting Model A") and model invariant energy export efficiency ("Limiting Model B").

"Limiting Model A": If all models had the same $ASR*$ value, then inter-model differences in MHT_{MAX} would be a direct consequence of inter-model differences in δ; models with more efficient meridional energy diffusion (B_{MHT}) or less efficient radiative exports (B_{OLR}) would have larger MHT_{MAX} values. MHT_{MAX} and $OLR*$ would be perfectly anti-correlated with a regression coefficient of negative 1.

"Limiting Model B": If B_{MHT} and B_{OLR} were model invariant but $ASR*$ differed between models, then MHT_{MAX} and $OLR*$ would be perfectly correlated with $ASR*$ (and each other) with the regression coefficients proportional to the relative magnitudes of $B_{MHT}$and B_{OLR} (and adding to unity). For example, if the dynamic energy export was 4 times more efficient than the radiative energy export in all models, then a model

with a 1 unit anomaly in ASR^* would be balanced 0.8 units of MHT_{MAX} anomaly and 0.2 units of OLR^* anomaly; the regression coefficient between the inter-model spread in MHT_{MAX} (OLR^*) would equal $\frac{\delta}{\delta+1}$ ($\frac{1}{\delta+1}$).

The large inter-model spread in ASR^* suggests that "Limiting Model A" is a poor fit to the inter-model spread in MHT_{MAX}. The correlation coefficients between MHT_{MAX}, OLR^*, and ASR^* (Table **??**) suggest that "Limiting Model B" is a descent, but far from perfect, description of the inter-model spread of MHT_{MAX}. We analyze these ideas more explicitly by plotting the inter-model spread of MHT_{MAX} in the ASR^*- $\frac{MHT_{MAX}}{ASR*}$ plane (Figure 1.1). MHT_{MAX} is the product of the axis and ordinate (the colored contours) and can be interpreted as the product of the model's ASR^* value and relative efficiency of dynamic heat transport to all energy export processes. The axis and ordinate have been scaled by equal fractions of the inter-model average so that the same spread on the axis and the ordinate correspond to equal magnitude differences in MHT_{MAX} (the gradient of MHT_{MAX} has unit slope). In the NH, the inter-model spread on the axis and ordinate are comparable (the black rectangular border surrounding the inter-model average represents a one standard deviation anomaly on each axis) suggesting that inter-model differences in ASR^* and energy export efficiencies contribute nearly equally to the spread in MHT_{MAX}. In the SH the spread on the axis exceeds that on the ordinate by approximately 50%, suggesting that model differences in ASR^* contribute more to the MHT_{MAX} spread than do differences in the energy export efficiencies. This framework presents an alternative view of the inter-model spread in MHT_{MAX} that can be reconciled with the statistics of ASR^* and OLR^* presented in Chapter 3. The key component is that models disagree substantially on the relative efficiency of dynamic and radiative energy exports (ordinate of Figure 1.1) but agree that dynamic energy export is a more efficient process. In the absence of ASR^* differences, models with more efficient dynamic heat transport have more MHT_{MAX} and less OLR^* ("Limiting Model A") and equal spread in OLR^* and MHT_{MAX}. In the absence of energy export efficiency differences ("Limiting Model B"), models with more ASR^* have more MHT_{MAX} and OLR^* but with the MHT_{MAX} difference anomaly approximately twice as large as the OLR^* anomaly (given by the inter-model average $\frac{\delta}{\delta+1}$). This process leads

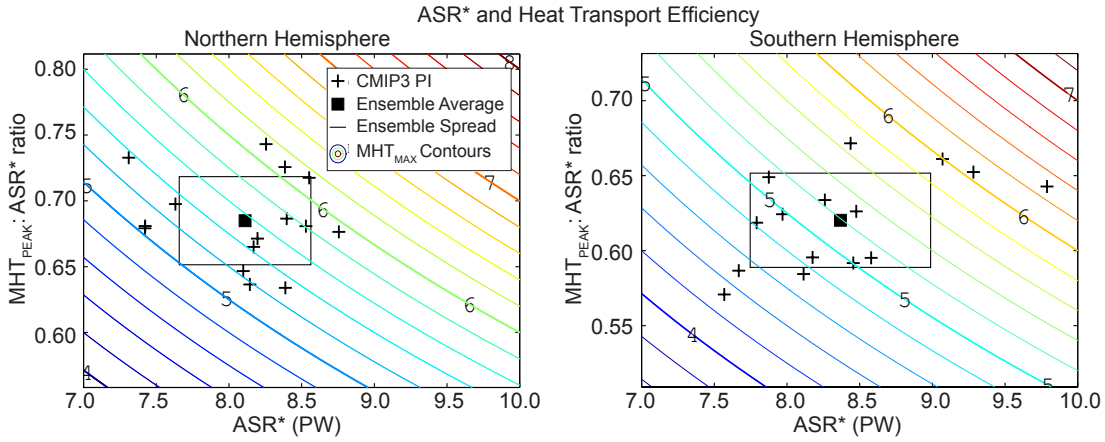

Figure 1.1: The ratio of MHT_{MAX}:$ASR*$ versus $ASR*$ for the CMIP3 PI simulations in the NH (left panel) and SH (right panel). The crosses are the individual models, the filled square is the ensemble average, and the hollow rectangular is one ensemble standard deviation on each axis. The colored contours are the MHT_{MAX} values.

to more MHT_{MAX} spread and less $OLR*$ spread as was seen in the CMIP3 ensemble (Table **??**). Therefore, the correlation between MHT_{MAX} and $ASR*$ seen in Chapter 3 is a consequence of the inter-model spread in $ASR*$ and an inter-model *average* δ value that is larger than 1. Inter-model variations in δ are significant and lead to a reduction of the correlations between $ASR*$ and MHT_{MAX} and also result in an insignificant correlation between MHT_{MAX} and $OLR*$.

The energy exports from the extra tropical climate system are analogous to a water tank that receives a constant inflow flux of water and losses water through two pipes of different diameters. In equilibrium, the inflow flux is equal to the sum of the outflow flux in both the pipes and the magnitude of the outflow flux in each pipe is proportional to the cross sectional area of the pipe. The outflow rate through any one of the pipes can be altered by either changing the inflow flux or changing the relative diameters of the two pipes. By analogy, $ASR*$ is akin to the inflow flux and B_{MHT} and B_{OLR} are akin to the cross sectional area of the pipes. Each climate model has a unique inflow rate and unique pipe diameters but all models agree that the MHT_{MAX} pipe has a larger diameter than the $OLR*$ pipe (the ordinate in Figure 1.1 is greater than 0.5). Therefore, inter-model differences in the

inflow rate will primarily be seen in the variations of the MHT_{MAX} outflow. Inter-model differences in the pipe diameters result in tradeoff between the two outflow fluxes with more water flowing through one pipe at the expense of less water flowing through the other pipe. The former process results in more inter-model spread in the outflow flux through the MHT_{MAX} pipe (as compared to the $OLR*$ outflow flux spread) where as the latter process results in equal (and anti-correlated) spread in both outflow fluxes. As a consequence of the concurrent inter-model spread of inflow rates and pipe diameters, there is more spread in the MHT_{MAX} outflow flux that is well correlated (but not perfectly correlated) with the inflow flux spread ($ASR*$ spread).

We now apply the concepts of energy export efficiency to the change in MHT_{MAX} due to CO_2 doubling (Figure 1.2). Similar to the inter-model spread, MHT_{MAX} can increase either by increasing the efficiency of dynamic energy export (or by decreasing the efficiency of radiative heat export) or by increasing $ASR*$. The orientation of the blue arrows connecting the PI simulations (black crosses) to the $2XCO_2$ simulations (red crosses) in the $ASR*$- $\frac{MHT_{MAX}}{ASR*}$ plane indicate whether changes in the relative magnitude of the dynamic and radiative energy export efficiencies or $ASR*$ contribute more ΔMHT_{MAX}; horizontal (vertical) arrows indicate that changes in $ASR*$ (heat export efficiencies) play a larger role in the MHT_{MAX} change.

In the NH, all the models indicate that dynamic energy exports become more efficient relative to the radiative energy exports in the $2XCO_2$ climate system (Soden and Held 2006). However, there is a large inter-model spread in $\Delta ASR*$ (Hwang and Frierson 2011) as can be seen from the ensemble average change (given by the thick blue arrow) and it's inter-model spread (1σ in each direction is given by the blue rectangle centered on the ensemble average change). The shift toward more efficient dynamic energy export is robust in the ensemble average (the blue rectangle does not intersect the PI inter-model average, given by the filled black square, along the ordinate) where as $\Delta ASR*$ is not significant (the blue rectangle crosses the PI inter-model average along the axis) and varies widely between models. As a consequence the inter-model average ΔMHT_{MAX} is not significantly different from zero as indicated by the overlap of the blue rectangle with the MHT_{MAX} contour value of the PI ensemble average (filled black square).

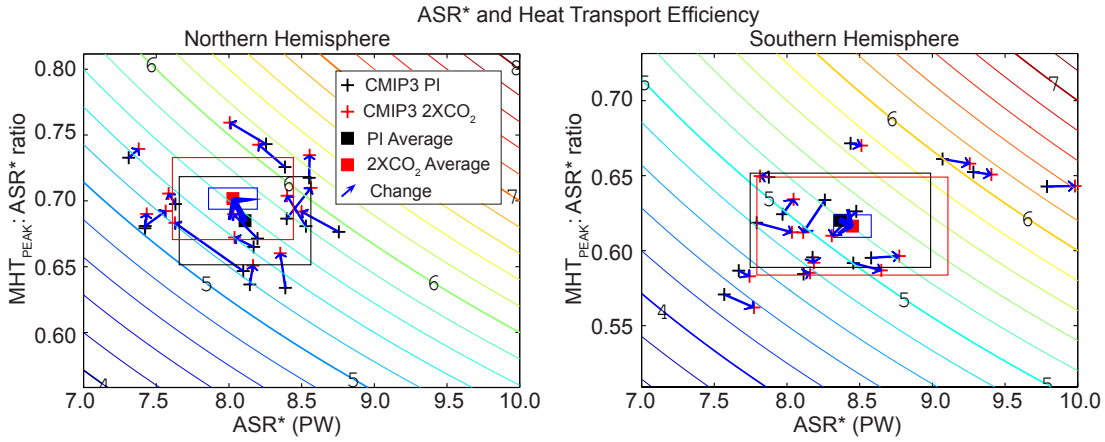

Figure 1.2: As in Figure 1.1 except with the addition of the $2XCO_2$ simulations (red crosses, square, and rectangle). The blue vectors indicate the change on each axis from the PI to the $2XCO_2$ simulation. The thick blue arrow is the ensemble average change and the blue rectangle gives one ensemble standard deviation of the change centered on the $2XCO_2$ ensemble average (red square).

In the SH, the ensemble average change in energy export efficiency and ASR^* are both insignificant, and the inter-model spread in ΔASR^* has a large impact on the spread in ΔMHT_{MAX} as compared to the energy export efficiency change. These results suggests the uncertainty ΔASR^* (due to cloud reflection changes) overwhelm any anticipated change in dynamic or radiative energy export efficiencies in terms of their affect on the change in meridional heat transport.

We started this thesis with a discussion of how analyzing large scale energy fluxes, both radiative and dynamic, across a multitude of spatio-temporal scales could provide further insight into the processes controlling the energy fluxes. This thesis has argued that the control of large scale energy fluxes can be thought of as a consequence of two bulk processes: (i) the processes controlling the spatio-temporal distribution of ASR and (ii) the relative efficiency of exporting energy between the regions and subcomponents of the climate system. We demonstrated that the ASR is controlled primarily by cloud properties and differs markedly between climate models. The relative efficiencies of energy exports are more constrained by fundamental physics (i.e. the Planck function is well established and

the heat capacity of the atmosphere contrains B_{CTEN} in all climate models); while there is some inter-model variability in the energy export efficiencies, all models agree on the ranking of the various processes. For example, all models have more efficient dynamic energy export on the equator-to-pole scale as compared to the radiative energy export and seasonal heat storage in the oceanic mixed layer is a more efficient energy sink for seasonal ASR than radiaitve or dynamic energy exports. Spatio-temporal gradients in ASR will adjust toward equilibrium along the most efficient pathway, and therefore, the relative partitioning of the global scale energy fluxes scales as the ASR structure times the relative export efficiency of a given process. Therefore, while the exact details of the energy flux parameterization in models do contribute to the inter-model spread in the magnitude of the energy fluxes, the vast majority of the inter-model spread is a consequence of the ASR spread and its partitioning along the most efficient dynamic energy pathway (MHT_{MAX} for the annual average equator-to-pole contrast problem).

In future work, we hope to apply these same ideas to the inter-model spread in the seasonal cycle and its change in altered climate states. We hope this work will continue to put the relative efficiency of dynamic and radiative energy exports into a common framework that is applicable across a multitude of spatio-temporal scales.